NASA/TM—2006-214462

Burst Testing and Analysis of Superalloy Disks With a Dual Grain Microstructure

John Gayda and Pete Kantzos
Glenn Research Center, Cleveland, Ohio

October 2006

NASA STI Program . . . in Profile

Since its founding, NASA has been dedicated to the advancement of aeronautics and space science. The NASA Scientific and Technical Information (STI) program plays a key part in helping NASA maintain this important role.

The NASA STI Program operates under the auspices of the Agency Chief Information Officer. It collects, organizes, provides for archiving, and disseminates NASA's STI. The NASA STI program provides access to the NASA Aeronautics and Space Database and its public interface, the NASA Technical Reports Server, thus providing one of the largest collections of aeronautical and space science STI in the world. Results are published in both non-NASA channels and by NASA in the NASA STI Report Series, which includes the following report types:

- TECHNICAL PUBLICATION. Reports of completed research or a major significant phase of research that present the results of NASA programs and include extensive data or theoretical analysis. Includes compilations of significant scientific and technical data and information deemed to be of continuing reference value. NASA counterpart of peer-reviewed formal professional papers but has less stringent limitations on manuscript length and extent of graphic presentations.

- TECHNICAL MEMORANDUM. Scientific and technical findings that are preliminary or of specialized interest, e.g., quick release reports, working papers, and bibliographies that contain minimal annotation. Does not contain extensive analysis.

- CONTRACTOR REPORT. Scientific and technical findings by NASA-sponsored contractors and grantees.

- CONFERENCE PUBLICATION. Collected papers from scientific and technical conferences, symposia, seminars, or other meetings sponsored or cosponsored by NASA.

- SPECIAL PUBLICATION. Scientific, technical, or historical information from NASA programs, projects, and missions, often concerned with subjects having substantial public interest.

- TECHNICAL TRANSLATION. English-language translations of foreign scientific and technical material pertinent to NASA's mission.

Specialized services also include creating custom thesauri, building customized databases, organizing and publishing research results.

For more information about the NASA STI program, see the following:

- Access the NASA STI program home page at *http://www.sti.nasa.gov*

- E-mail your question via the Internet to *help@sti.nasa.gov*

- Fax your question to the NASA STI Help Desk at 301–621–0134

- Telephone the NASA STI Help Desk at 301–621–0390

- Write to:
  NASA STI Help Desk
  NASA Center for AeroSpace Information
  7121 Standard Drive
  Hanover, MD 21076–1320

NASA/TM—2006-214462

Burst Testing and Analysis of Superalloy Disks With a Dual Grain Microstructure

John Gayda and Pete Kantzos
Glenn Research Center, Cleveland, Ohio

National Aeronautics and
Space Administration

Glenn Research Center
Cleveland, Ohio 44135

October 2006

Trade names and trademarks are used in this report for identification only. Their usage does not constitute an official endorsement, either expressed or implied, by the National Aeronautics and Space Administration.

Level of Review: This material has been technically reviewed by technical management.

Available from

NASA Center for Aerospace Information
7121 Standard Drive
Hanover, MD 21076–1320

National Technical Information Service
5285 Port Royal Road
Springfield, VA 22161

Available electronically at http://gltrs.grc.nasa.gov

Burst Testing and Analysis of Superalloy Disks With a Dual Grain Microstructure

John Gayda and Pete Kantzos
National Aeronautics and Space Administration
Glenn Research Center
Cleveland, Ohio 44135

Introduction

As operating temperatures of gas turbine engines increase, there is a need for superalloy turbine disks which can operate with rim temperatures in excess of 1300 °F. To meet this need, a new generation of nickel-base superalloys, such as Rene 104 (initially designated ME3, General Electric Aircraft Engines), Alloy 10 (Honeywell Engines & Systems), and Low Solvus High Refractory (LSHR), have been developed (refs. 1 to 3). These alloys all contain a high percentage of gamma prime precipitates, Ni_3Al, and refractory element additions to achieve strength at temperature. Although they provide advantages over older alloys, the continuing need for high tensile strength at intermediate temperatures in the bore of a disk, which runs much cooler than the rim, as well as high creep strength in the rim also demands innovative heat treatments which can optimize bore and rim properties. Traditional heat treatments produce fine grain disks when the solution temperature is maintained below the gamma prime solvus, or coarse grain disks when the solution temperature is maintained above the gamma prime solvus. Fine grain disks yield high strength at intermediate temperatures, while coarse grain disks yield high creep strength at elevated temperatures. Recently, several advanced heat treatment technologies (refs. 4 to 6) have been developed which can produce a superalloy disk with fine grain bore and coarse grain rim. Trade studies by General Electric Aircraft Engines (GEAE) (ref. 7) and Allison Advanced Development Company (AADC) (ref. 8) have identified potential advantages offered by superalloy disks which employ a dual grain structure for advanced gas turbine engine application. The GEAE report cited a fatigue benefit for a disk with a dual grain structure when compared with a coarse grain disk, while the AADC report cited a creep benefit for a disk with a dual grain structure when compared with a fine grain disk.

A two year program between AADC, GEAE, and NASA was undertaken to develop/refine design methodologies for yield and burst criteria of superalloy disks with dual grain structures. Previous spin testing of disks with dual grain structures were conducted to rigorously test the integrity of the grain size transition zone with unusually high web stresses. In this study, room temperature burst testing and analysis of four superalloy disks were performed with moderate web stresses more typical of real production disks in gas turbine engines. AADC chose to study Alloy 10 disks with a dual grain structure and a uniform fine grain structure. GEAE chose to study Rene 104 disks with a dual grain structure and a uniform coarse grain structure. The chose of alloy and disk microstructure comparison reflected current design interest of each company. A final report on testing and analysis by each company can be found in references 9 and 10. The purpose of this report is to compare the results of all four burst tests using a common analysis run by NASA which employed a simplified elastic-plastic finite element technique.

Materials and Procedures

In this program a generic disk shape based on AADC's AE2100 stage-3 turbine disk, nominally 14 in. in diameter and 2 in. thick, was employed as depicted in figure 1. The disks were isothermally forged by the Ladish Company using extruded mults of Alloy 10 and Rene 104 supplied by AADC and GEAE, respectively. After forging, the Ladish Company heat treated the Alloy 10 forgings producing two disks with a dual grain structure and one disk with a uniform fine grain structure, ASTM 11-12. The disks with a dual grain microstructure were produced using NASA's patented Dual Microstructure Heat Treatment (DMHT) process (ref. 6). GEAE chose to have the Rene 104 forgings heat treated at the Wyman-Gordon

facility in Houston, Texas. Two dual grain structure disks were produced using GEAE's patented process (ref. 5) and a third disk was processed to produce a uniform coarse grain structure, ASTM 7. The transition radius of the Alloy 10 dual grain structure disk was determined to be 5.3 in. while that of the Rene 104 dual grain structure disk was determined to be 4.5 in., both in line with expectations. The bore/rim sections of the dual grain structure disks had a grain size of ASTM 11/6 and ASTM 12/5 for the Alloy 10 and Rene 104, respectively. More details on the processing history and resulting microstructures can be found in the individual contractor reports (refs. 9 and 10).

After heat treatment, one of the Alloy 10 and Rene 104 disks with the dual grain structure were sectioned to provide tensile, notch tensile, and fatigue test bars. The cut-up plan and test results are documented in the contractor reports. Room temperature tensile data used in the subsequent NASA analysis is summarized in table I. The remaining disks were machined by Douglas Machining of Evendale, Ohio using the machining plan shown in figure 2. As seen in this figure the final disk shape was designed with rim slot features to simulate blade loading. This design was intended to produce the highest stresses, and therefore failure at the bottom of the rim holes. For both the Alloy 10 and Rene 104 disks, the critical location was outboard of the transition zone well into the coarse grain region of the disks with the dual grain structure. After machining at Douglas, each company was free to pursue any inspection or any additional surface treatment deemed critical for their alloy. A photo of a machined disk is presented in figure 3 after acceptance by both companies.

Room temperature spin testing of the four machined disks was performed by Test Devices, Inc. of Hudson, Massachusetts. During each test, the disk was connected to the air turbine/spindle drive via a stainless steel arbor attached to the bore flange on the disk with 24 bolts. Radial proximity probes were used to monitor disk growth to failure. High speed video and eight channels of strain data were recorded in each test as described in the contractor reports (refs. 9 and 10). Redundant strain gages (2) were employed at the critical disk location, i.e., bottom of rim holes at the 0 and 180° position. A photo of the spin pit with the disk is presented in figure 4.

Experimental Results

Each of the four spin tests were run in three segments. During the first segment the disk was spun to a maximum speed of 21000 rpm before returning to rest. At this speed, the response of all four disks was intended and found to be largely elastic, as strain gage and proximity probe data returned to near-zero readings upon completion. The response, of all four disks for this segment of the tests, is summarized in table II. As expected the strain gage at the bottom of the rim hole produced the largest strain.

For the next test segment, the disks were spun to a maximum speed which produced 3 percent total strain at the bottom of the rim hole before returning to rest. The resulting readings at maximum speed and rest for all four disks are summarized in table III. Significant flow and growth of the disks are evident by non-zero readings upon completion of this test segment.

The final test segment, for all four disks, was run to burst. As most of the strain gage signals were lost before burst, only the burst speeds and radial growth are presented in table IV. High speed video clearly showed failure initiated from the base of the rim holes in all tests. A series of photos showing the progression of crack propagation for one of the tests is shown in figure 5. As seen in table IV, the Rene 104 burst speeds and radial growth data were significantly higher than that for Alloy 10. Further, the burst speed for the dual grain Rene 104 disk was greater than that of the coarse grain Rene 104 disk, while the burst speed for the dual grain Alloy 10 disk was less than that of the fine grain Alloy 10 disk.

Finite Element Analysis

To understand and compare the results of all four spin tests, NASA utilized a simplified finite element analysis employing a commercial platform from Algor, Inc., MES with Nonlinear Material Models Version 12.28. As all tests were conducted at room temperature to burst, an elastic-plastic, bilinear material model with isotropic hardening was employed using the data presented in table I. When an

element's von Mises stress exceeded the yield strength, its stiffness was set equal to a plastic modulus, which was defined by the following formula:

$$E_{plastic} = (\text{Ultimate Tensile Strength-Yield Strength})/\text{Tensile Elongation}$$

The disks with dual grain structures were divided into two material groups. Inside the transition zone fine grain properties were employed. Outside the transition zone coarse grain properties were employed. The three-dimensional meshed model of a dual grain disk is presented in figure 6. The analysis mimicked the three test segments, i.e., the disk was spun to 21000 rpm, unloaded, spun to 3 percent rim strain, unloaded, and finally spun to burst. Analytically, disk burst was assumed to occur when the von Mises stress equaled the ultimate tensile strength of the alloy. As expected this occurred at the base of the rim holes in all analyses, a typical run is shown in figure 7. Comparative plots of the radial growth for all four disks, based on the aforementioned analysis procedure, are presented in figure 8 showing all test segments. Note that the time scale is artificial and was chosen for analytical convenience as the elastic-plastic analysis employed in this study yields a time-independent solution. The peak values in these plots do, however, correspond to maximum and zero rpm levels in the three segment test procedure. All four analyses showed very little plastic flow after segment 1, loading to 21000 rpm, and significant plastic flow after segment 2, loading to 3 percent strain at the base of rim holes, as evident by the level of permanent radial growth after unloading to zero rpm. The maximum speed and radial growth of the final segment was determined using an iterative process, that is, the maximum rpm was varied until the von Mises stress at the base of the rim hole equaled the ultimate tensile strength of the alloy.

A comparison between the analytical and experimental growth rates of all four disks is presented in figure 9. The predicted growth rates prior to burst are fairly accurate for all tests considering the simplifying assumptions used in the analysis. However, the differences in growth at burst between experiment and analysis as well as between the alloys are significant. Analytically the predicted differences in growth at burst are relatively modest between all four disks, with a low of 0.086 in. and a high of 0.103 in., the experimental data however, shows the Rene 104 disks averaging about 0.14 in., which is significantly higher than the Alloy 10 disks which averaged about 0.07 in. Looking at the same data from another perspective, the analytical growth rate at burst of the Alloy 10 disks are greater than the experimental data, while the analytical growth rate at burst of the Rene 104 disks are less than the experimental data. A comparison of analytical and experimental burst speeds of all four disks is presented in table V. As with growth at burst, the predicted burst speeds show only modest differences, high of 25200 rpm for fine grain Alloy 10 and a low of 24800 rpm for coarse grain Rene 104, while the experimental results, as previously stated, show the Rene 104 disks to have failed at significantly higher speeds than the Alloy 10 disks. Taken as a whole, the burst data, both growth and speed, suggest differences in alloy behavior were more pronounced than differences between heat treat option, i.e. dual grain versus uniform grain structure. Finally, it should be noted, for each alloy the ranking of burst speed between dual grain and uniform grain structure was correctly predicted. The burst speed for fine grain Alloy 10 was greater than dual grain Alloy 10, and the burst speed for coarse grain Rene 104 was less than dual grain Rene 104.

Fractographic Analysis

Failure analysis of the burst disks was performed in order to confirm failure locations and to determine possible differences in failure modes or microstructure that may explain the observed discrepancies in behavior between the alloys. The failed disks were reconstructed as shown in figure 10. With the aid of the high speed test video and paint pattern on the disk, the initiation location and progression of failure was identified. As expected, all disks failures initiated at the root of the rim hole. Fractography of several primary and secondary initiation sites on all the disks revealed that a common location of failure was approximately 4 mm from the bottom of the disk (fig. 11). The conjugate location

from the top side of the disk was also a prevalent initiation site. As shown in figure 11, the failure location was accurately predicted by the three-dimensional elasto-plastic FEA models generated by both GEAE and AADC.

The failure mode for both alloys was typical of tensile fracture as shown in figure 12. Also, none of the initiation sites, primary or secondary, revealed any material related defects that may have attributed to the observed differences in burst behavior. Furthermore, metallography did not reveal any abnormal microstructure. The disk grain sizes in the region were failure occurred were also as expected for both alloys and heat treatments. One obvious difference was the deformation present at the surface of the hole for the Alloy 10 DMHT disk (fig. 13). (This type of localized surface deformation is likely to represent cold work from a machining operation.) The R104 disks did not show any surface deformation. Subsequent examination of the surface of intact rim holes adjacent to holes that initiated failure also revealed differences in the nature and extent of damage. As seen in figure 14, in comparison to the R104 DMHT disk, the Alloy 10 DMHT disk revealed significantly more microcracking. Furthermore, most of the microcracks in the Alloy 10 disk have coalesced into long cracks. This behavior may be a manifestation of surface cold work suggesting lack of ductility and premature cracking. Since only the surface material is deformed, the premature cracking was limited to the surface layer. Premature surface cracking, even if shallow, can hasten the failure process and may explain the smaller radial growth at burst observed for the Alloy 10 disks.

Summary and Conclusions

Elastic-plastic finite element analyses of room temperature burst tests on four superalloy disks were conducted and reported in this paper. Two alloys, Rene 104 and Alloy 10, were studied. For both alloys an advanced dual microstructure disk, fine grain bore and coarse grain rim, were analyzed and compared with conventional disks with uniform microstructures, coarse grain for Rene 104 and fine grain for Alloy 10. The analysis and experimental data were in good agreement up to burst. At burst, the analysis underestimated the speed and growth of the Rene 104 disks, but overestimated the speed and growth of the Alloy 10 disks. Fractography revealed that the Alloy 10 disks displayed significant surface microcracking and coalescence in comparison to Rene 104 disks. This phenomenon may help explain the differences between the Alloy 10 disks and the Rene 104 disks, as well as the observed deviations between analytical and experimental data at burst.

In conclusion, this work, coupled with previous efforts by NASA, extends DMHT maturity to a level where industry can utilize this technology in advanced engine designs. Both the performance and analysis capability for DMHT technology is firmly established and documented.

References

1. T. Gabb, J. Telesman, P. Kantzos, and K. O'Connor, "Characterization of the Temperature Capability of Advanced Disk Alloy ME3," NASA/TM—2002-211796, August 2002.
2. S. Jain, "Regional Engine Disk Process Development," NASA Contract NAS3–27720, September 1999.
3. T. Gabb, J. Gayda, J. Telesman, "Realistic Subscale Evaluation of the Mechanical Properties of Advanced Disk Superalloys," NASA/TM—2003-212086, January 2003.
4. G. Mathey, "Method of Making Superalloy Turbine Disks Having Graded Coarse and Fine Grains," U.S. Patent 5,312,497, May 17, 1994.
5. S. Ganesh and R. Tolbert, "Differentially Heat Treated Article and Apparatus and Manufacture Thereof," U.S. Patent 5,527,020, June 18, 1996.
6. J. Gayda, T. Gabb, and P. Kantzos, "Heat Treatment Technology for Production of Dual Microstructure Superalloy Disks," NASA/TM—2002-211558, April 2002.
7. J. Williams, "Dual Heat Treat Superalloy Disk Design Trade Study," NASA/CR—2004-212949, February 2004.

8. K. Green, “Trade Study on Dual Microstructure Heat Treat Technology,” NASA/CR—2004-212948, February 2004.
9. T. Heffernan, “Spin Testing of Superalloy Disks with Dual Grain Structure,” NASA/CR—2006-214338, May 2006.
10. J. Groh, “Spin Test of Superalloy Disks with Dual Grain Structure,” NASA/CR—2006-214266, April 2006.

TABLE I.—TENSILE DATA USED IN CURRENT ANALYSIS
[Bore is fine grain and rim is coarse grain.]

Rene 104	Yield (ksi)	UTS (ksi)	E (msi)	Elong	Density (lb/in.^{3})
Bore	170	244	32	24 percent	0.3
Rim	160	230	32	20 percent	0.3

Alloy 10	Yield (ksi)	UTS (ksi)	E (msi)	Elong	Density (lb/in.^{3})
Bore	165	240	32	25 percent	0.3
Rim	155	225	32	23 percent	0.3

TABLE II.—EXPERIMENTAL DATA FOR FIRST TEST SEGMENT TO 21000 RPM
[Negligible growth and strains measured upon unloading to zero rpm.]

	Coarse grain Rene 104	Dual grain Rene 104	Fine grain Alloy 10	Dual grain Alloy 10
Growth	0.016 in.	0.014 in.	0.009 in.	0.010 in.
Bore strain	0.6 percent	0.8 percent	0.6 percent	0.6 percent
Web strain	0.3 percent	0.3 percent	0.3 percent	0.3 percent
Rim strain	0.8 percent	0.7 percent	0.7 percent	0.8 percent

TABLE III.—EXPERIMENTAL DATA FOR SECOND TEST SEGMENT TO 3 PERCENT TARGET RIM STRAIN
[Data denoted with (1) refers to measurement at max speed and data denoted with (2) refers to measurements upon unloading to zero rpm.]

	Coarse grain Rene 104	Dual grain Rene 104	Fine grain Alloy 10	Dual grain Alloy 10
Max Speed	23 400 rpm	23 600 rpm	23 600 rpm	23 300 rpm
Growth (1)	0.038 in.	0.030 in.	0.028 in.	0.021 in.
Growth (2)	0.014 in.	0.012 in.	0.012 in.	0.007 in.
Bore (1)	1.3 percent	1.5 percent	1.5 percent	1.0 percent
Bore (2)	0.6 percent	----------	0.8 percent	0.2 percent
Web (1)	0.7 percent	0.9 percent	0.8 percent	0.8 percent
Web (2)	0.1 percent	0.1 percent	0.4 percent	0.3 percent
Rim (1)	2.8 percent	2.5 percent	3.0 percent	3.0 percent
Rim (2)	1.8 percent	----------	----------	2.1 percent

TABLE IV.—EXPERIMENTAL DATA FOR THIRD TEST SEGMENT TO BURST

	Coarse grain Rene 104	Dual grain Rene 104	Fine grain Alloy 10	Dual grain Alloy 10
Burst speed	24 670 rpm	25 030 rpm	24 240 rpm	24 005 rpm
Growth	0.147 in.	0.137 in.	0.068 in.	0.067 in.

TABLE V.—COMPARISON OF PREDICTED AND MEASURED BURST SPEEDS

	Coarse grain Rene 104, rpm	Dual grain Rene 104, rpm	Fine grain Alloy 10, rpm	Dual grain Alloy 10, rpm
Predicted	24 800	25 100	25 200	24 800
Measured	24 670	25 030	24 240	24 005

Figure 1.—Forged shape of disk.

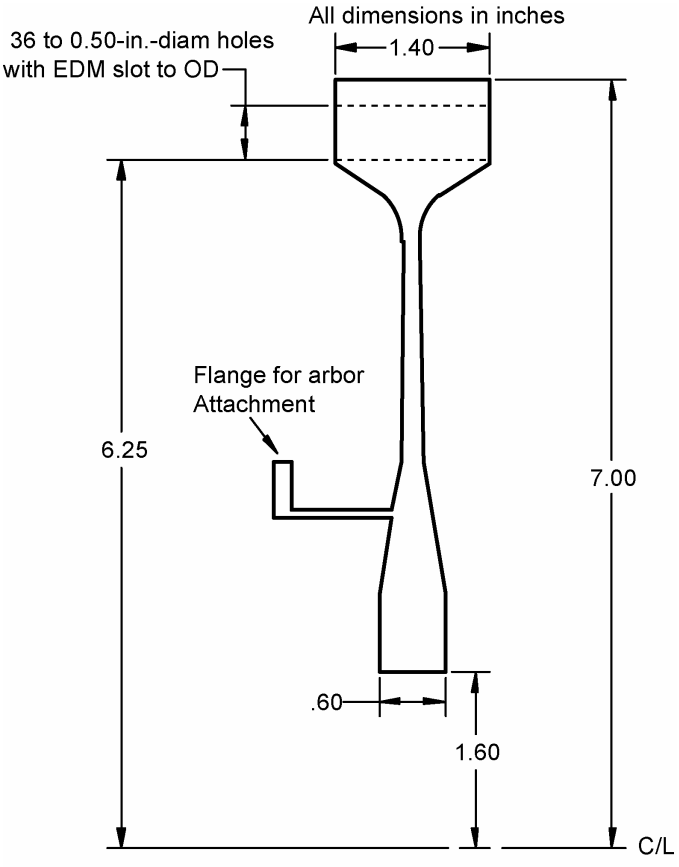

Figure 2.—Machining plan for disk showing critical dimensions.

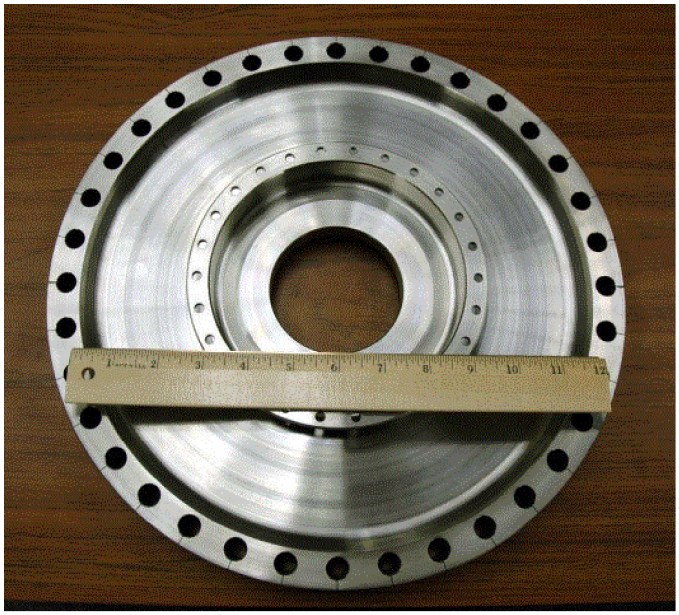

Figure 3.—Photo of machined disk.

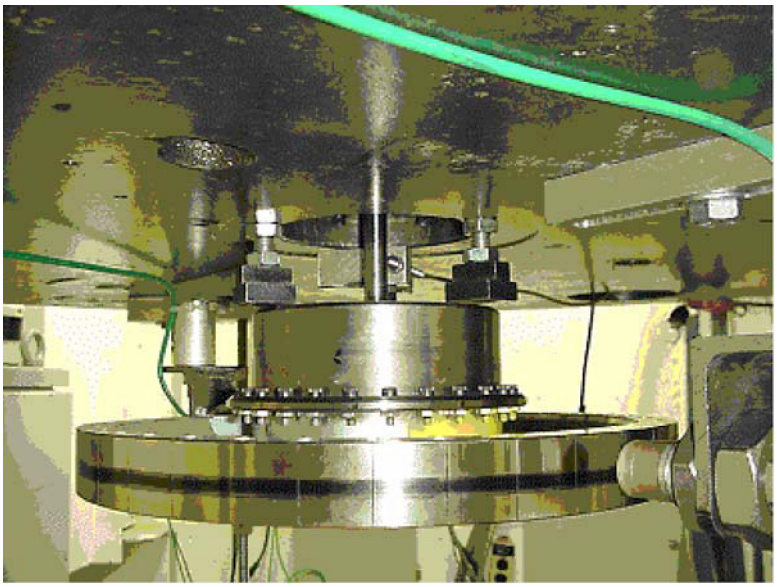

Figure 4.—Photo of disk in spin pit.

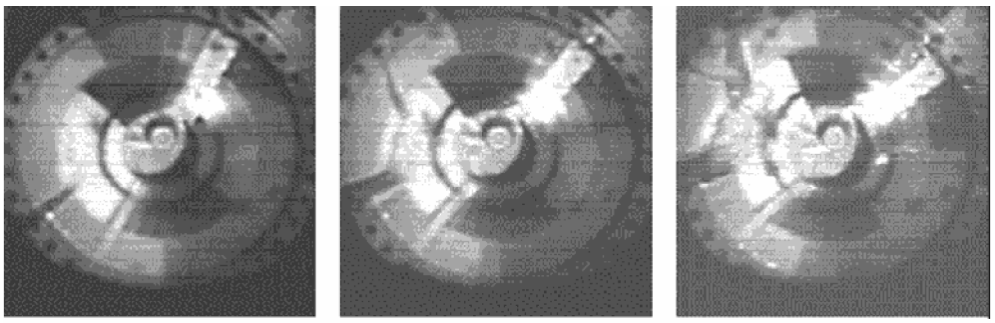

Figure 5.—Photos from high speed video showing disk burst.

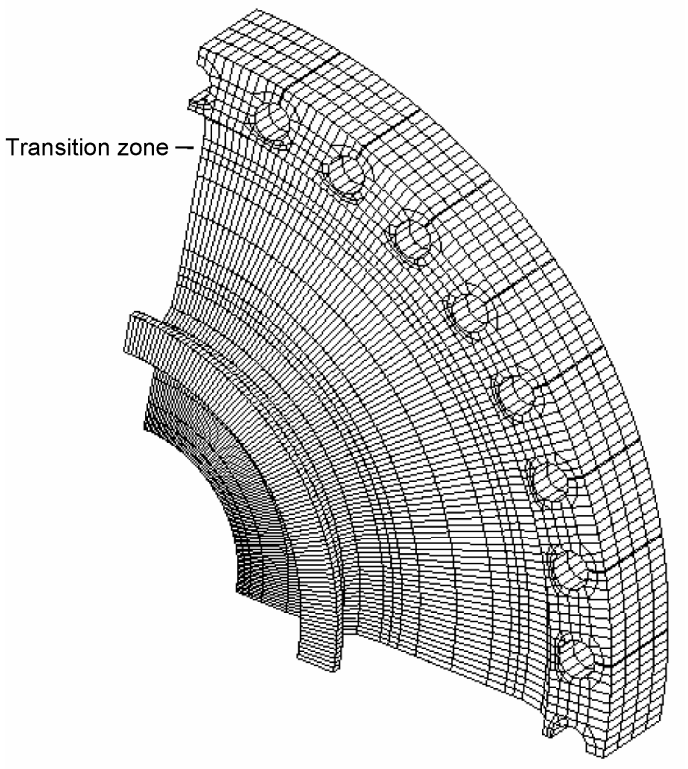

Figure 6.—Meshed model of disk employed in this analysis.

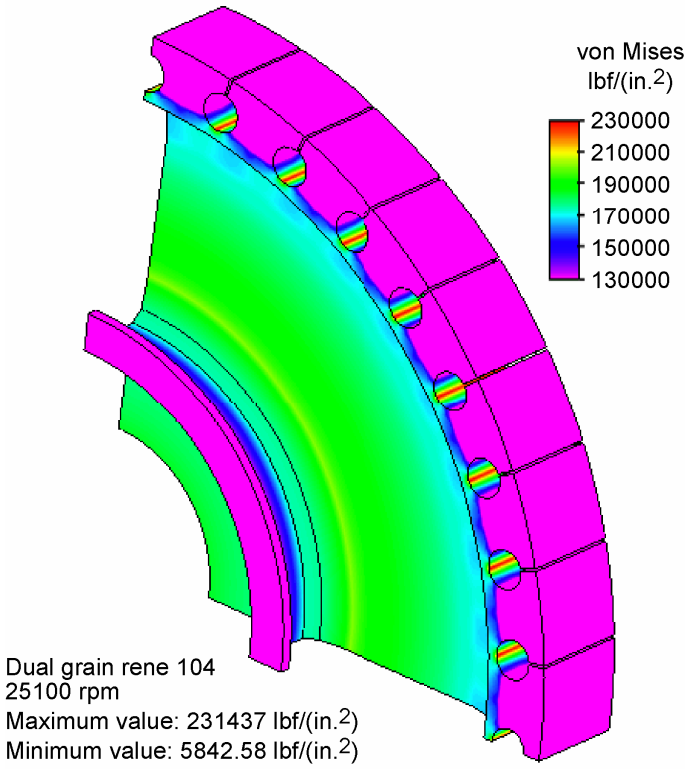

Figure 7.—Predicted von Mises stress distribution in dual grain Rene 104 at burst.

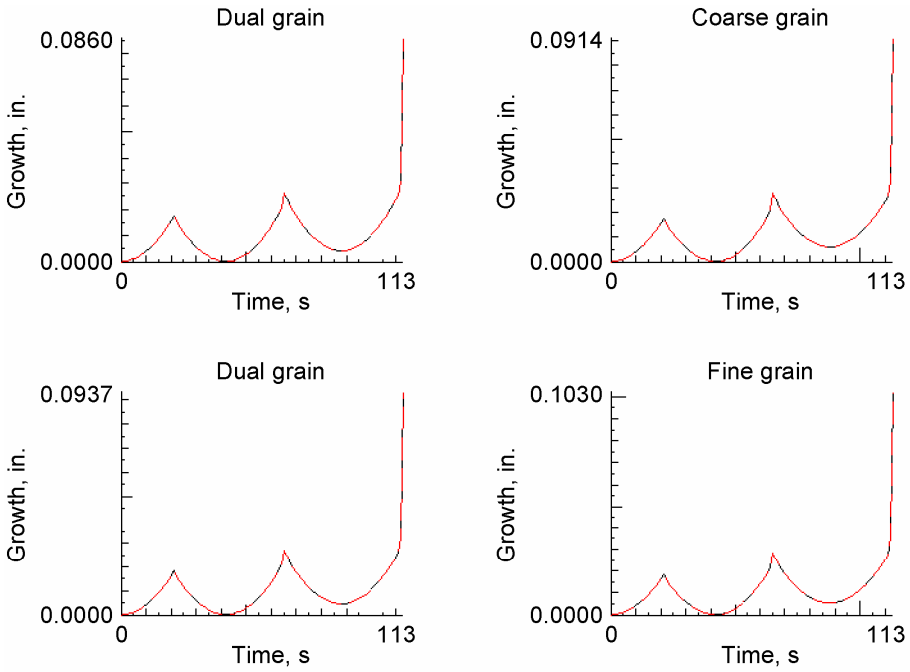

Figure 8.—Predicted radial growth curves (inches). Rene 104 results on top and Alloy 10 results on bottom.

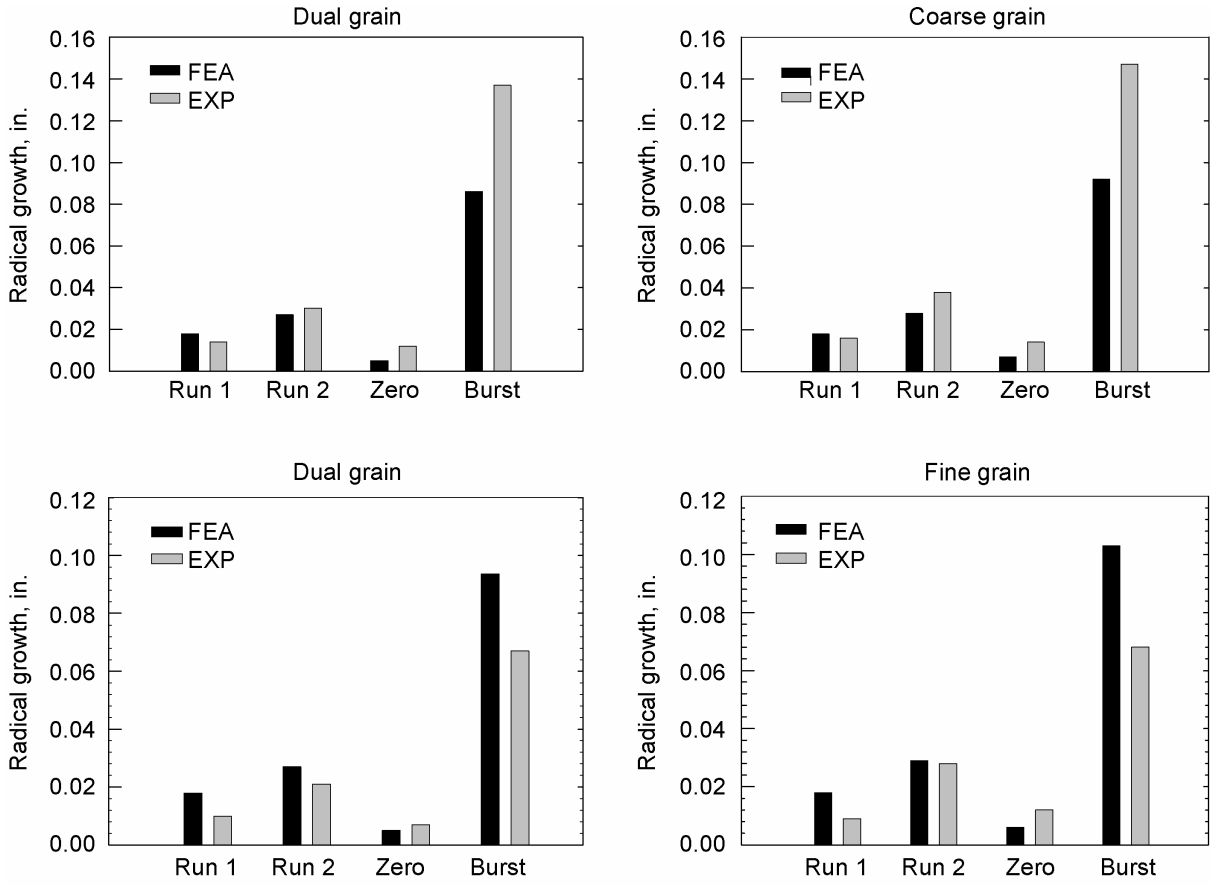

Figure 9.—Comparison of experimental (EXP) and analytical (FEA) growth rates. Rene 104 data on top and Alloy 10 data on bottom.

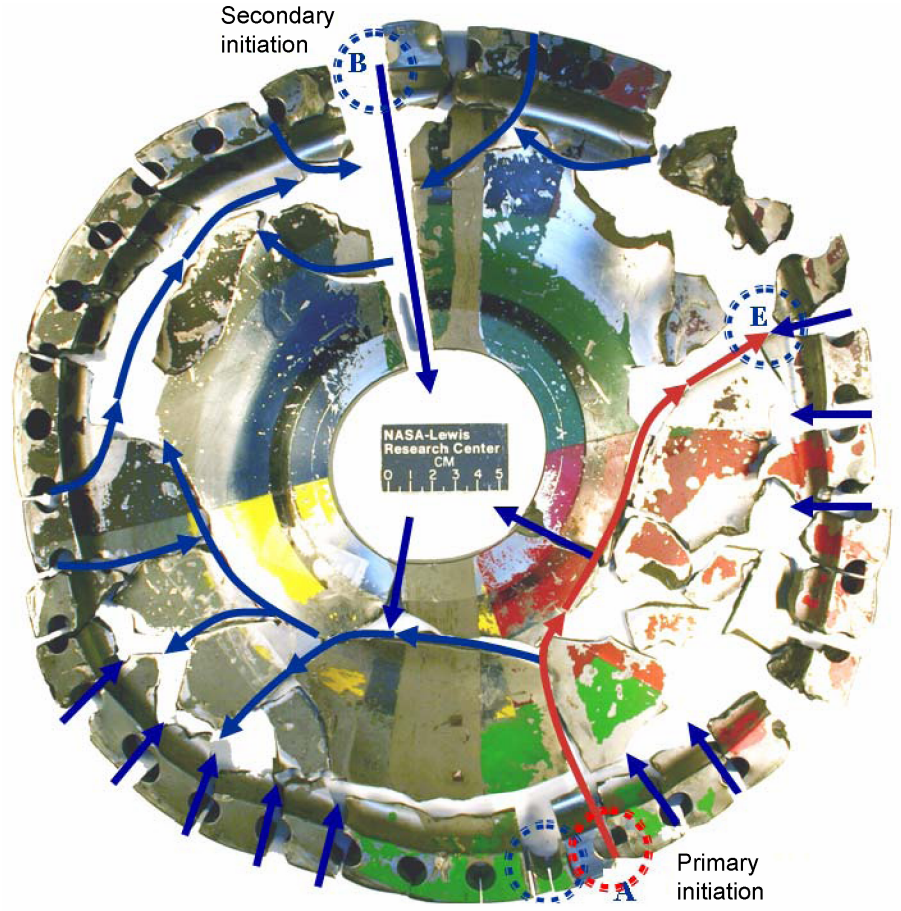

Figure 10.—Rene104 DMHT disk reconstructed showing the primary and secondary initiations and general failure path.

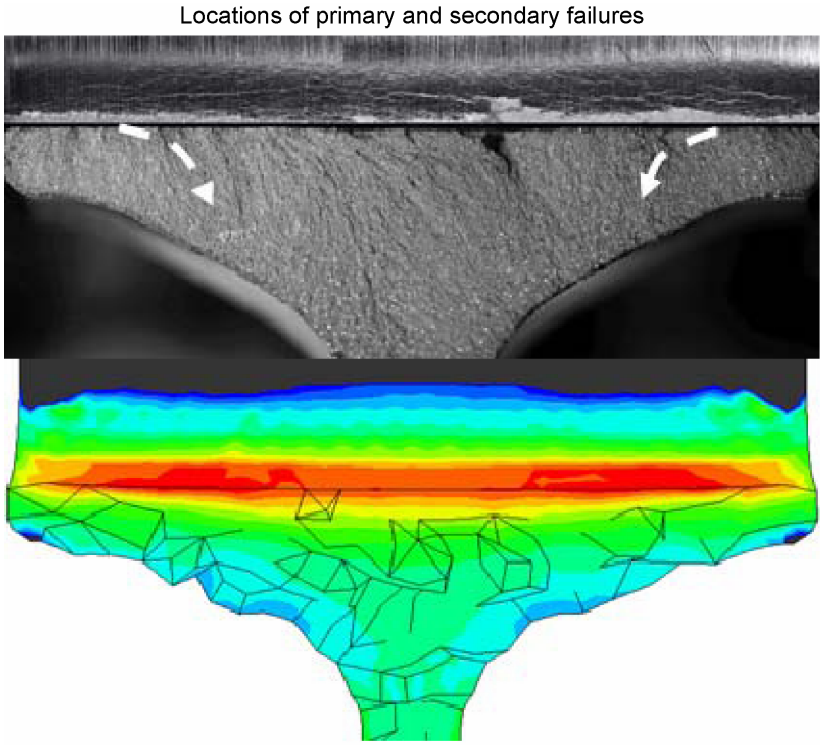

Figure 11.—Rim hole where the primary initiation occurred for Alloy10 DMHT disk. The arrows indicate the preferred location for failure initiation which corresponds well with the location predicted by the stress analysis (courtesy of D. Thomas from AADC.)

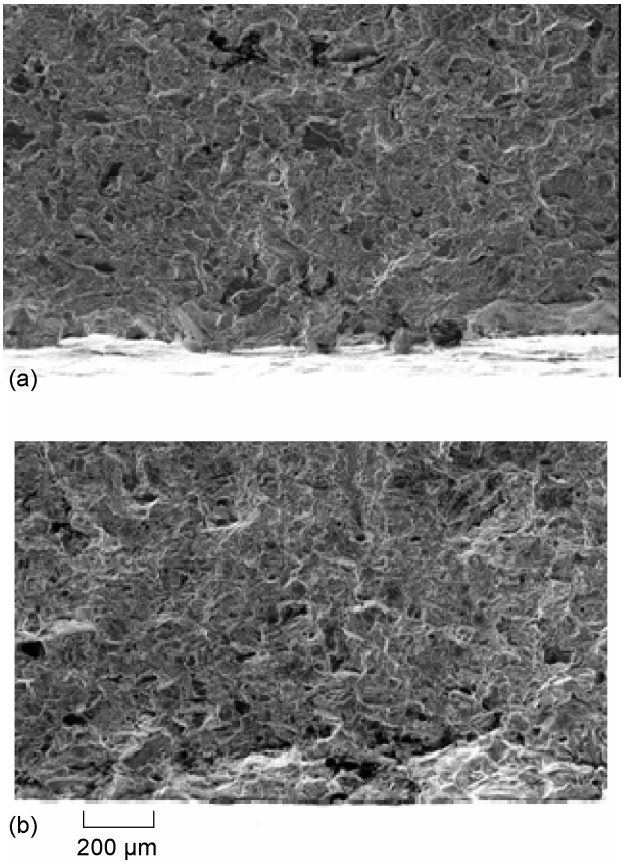

Figure 12.—Typical initiation locations for (a) Rene 104 and (b) Alloy10 DMHT disks.

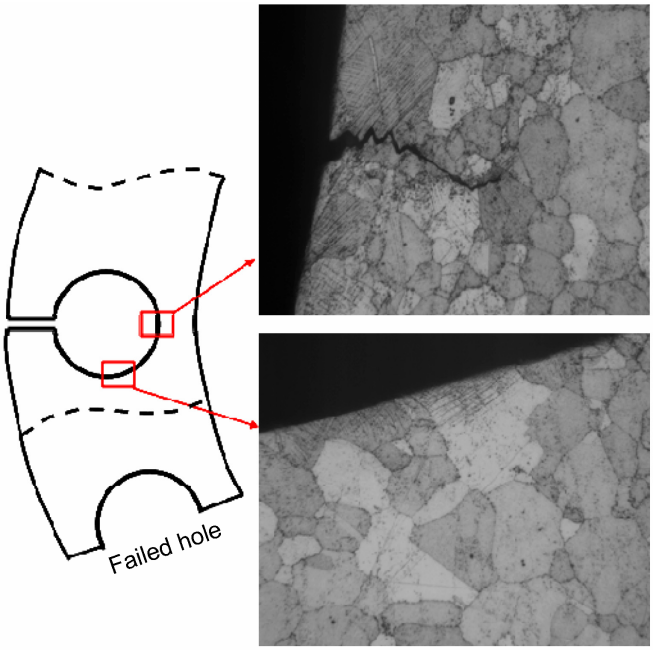

Figure 13.—Surface deformation observed on machined rim hole of Alloy10 DMHT disk.

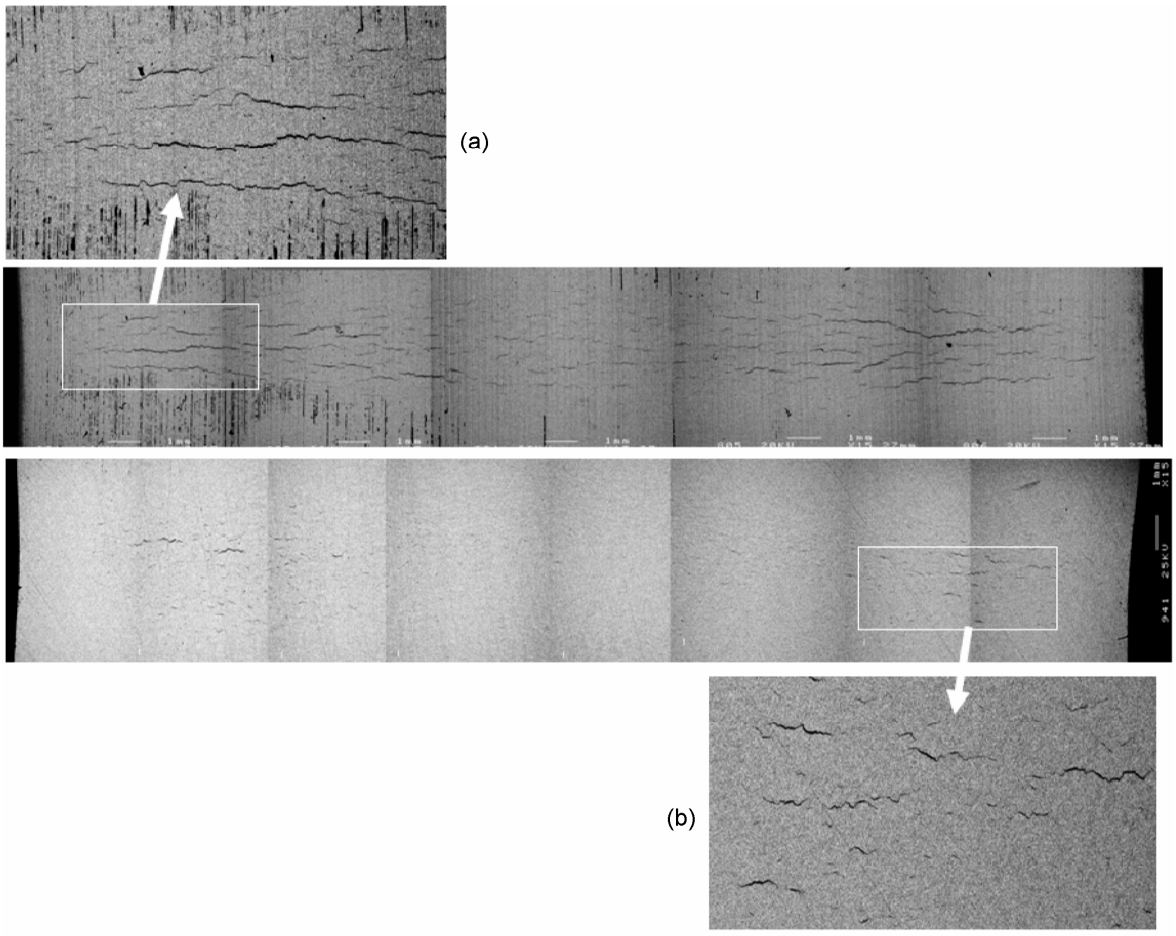

Figure 14.—Comparison of micro-cracking behavior of intact rim holes in (a) Alloy10 DMHT disk and (b) Rene 104 DMHT disks.

REPORT DOCUMENTATION PAGE

Form Approved
OMB No. 0704-0188

Public reporting burden for this collection of information is estimated to average 1 hour per response, including the time for reviewing instructions, searching existing data sources, gathering and maintaining the data needed, and completing and reviewing the collection of information. Send comments regarding this burden estimate or any other aspect of this collection of information, including suggestions for reducing this burden, to Washington Headquarters Services, Directorate for Information Operations and Reports, 1215 Jefferson Davis Highway, Suite 1204, Arlington, VA 22202-4302, and to the Office of Management and Budget, Paperwork Reduction Project (0704-0188), Washington, DC 20503.

1. AGENCY USE ONLY (*Leave blank*)	2. REPORT DATE	3. REPORT TYPE AND DATES COVERED
	October 2006	Technical Memorandum

4. TITLE AND SUBTITLE

Burst Testing and Analysis of Superalloy Disks With a Dual Grain Microstructure

5. FUNDING NUMBERS

WBS 698259.02.07.03

6. AUTHOR(S)

John Gayda and Pete Kantzos

7. PERFORMING ORGANIZATION NAME(S) AND ADDRESS(ES)

National Aeronautics and Space Administration
John H. Glenn Research Center at Lewis Field
Cleveland, Ohio 44135–3191

8. PERFORMING ORGANIZATION REPORT NUMBER

E–15726

9. SPONSORING/MONITORING AGENCY NAME(S) AND ADDRESS(ES)

National Aeronautics and Space Administration
Washington, DC 20546–0001

10. SPONSORING/MONITORING AGENCY REPORT NUMBER

NASA TM—2006-214462

11. SUPPLEMENTARY NOTES

Responsible person, John Gayda, organization code RXA, 216–433–3273.

12a. DISTRIBUTION/AVAILABILITY STATEMENT

Unclassified - Unlimited
Subject Category: 26

Available electronically at http://gltrs.grc.nasa.gov

This publication is available from the NASA Center for AeroSpace Information, 301–621–0390.

12b. DISTRIBUTION CODE

13. ABSTRACT ***(Maximum 200 words)***

Elastic-plastic finite element analyses of room temperature burst tests on four superalloy disks were conducted and reported in this paper. Two alloys, Rene 104 (General Electric Aircraft Engines) and Alloy 10 (Honeywell Engines & Systems), were studied. For both alloys an advanced dual microstructure disk, fine grain bore and coarse grain rim, were analyzed and compared with conventional disks with uniform microstructures, coarse grain for Rene 104 and fine grain for Alloy 10. The analysis and experimental data were in good agreement up to burst. At burst, the analysis underestimated the speed and growth of the Rene 104 disks, but overestimated the speed and growth of the Alloy 10 disks. Fractography revealed that the Alloy 10 disks displayed significant surface microcracking and coalescence in comparison to Rene 104 disks. This phenomenon may help explain the differences between the Alloy 10 disks and the Rene 104 disks, as well as the observed deviations between analytical and experimental data at burst.

14. SUBJECT TERMS	15. NUMBER OF PAGES
Superalloy disks	20
	16. PRICE CODE

17. SECURITY CLASSIFICATION OF REPORT	18. SECURITY CLASSIFICATION OF THIS PAGE	19. SECURITY CLASSIFICATION OF ABSTRACT	20. LIMITATION OF ABSTRACT
Unclassified	Unclassified	Unclassified	